Three-dimensional spiral waves in an excitable reaction system: Initiation and dynamics of scroll rings and scroll ring pairs

Tamás Bánsági, Jr. and Oliver Steinbock[a)]
Department of Chemistry and Biochemistry, Florida State University, Tallahassee, Florida 32306-4390, USA

(Received 2 January 2008; accepted 19 February 2008; published online 27 June 2008)

We report experimental results on spiral and scroll waves in the 1,4-cyclohexanedione Belousov–Zhabotinsky reaction. The propagating concentration waves are detected by two-dimensional photometry and optical tomography. Wave pulses can disappear in front-to-front and front-to-back collisions. This anomaly causes the nucleation of vortices from collisions of three nonrotating waves. In three-dimensional systems, these vortices are scroll rings that rotate around initially circular filaments. Depending on reactant concentrations, the filaments shrink or expand indicating positive and negative filament tensions, respectively. Shrinkage results in vortex annihilation. Expansion is accompanied by filament buckling and bending, which is interpreted as developing Winfree turbulence. We also describe the initiation of scroll ring pairs in four-wave collisions. The two filaments are stacked on top of each other and their motion suggests filament repulsion. © *2008 American Institute of Physics*. [DOI: 10.1063/1.2896100]

Spiral waves of excitation exist in a variety of experimental systems including chemical reaction-diffusion media, living cells, and cellular tissues. In two space dimensions, their shape is close to that of an Archimedean spiral. Their tip orbits along a simple, often circular, trajectory. The spiral analog in three dimensions is the scroll wave which rotates around dynamic, one-dimensional space curves. A specific case is the scroll ring for which the filament is a closed loop. The latter curve shrinks or expands according to the system's filament tension. We report an experimental study of scroll rings in a chemical reaction solution which can generate positive as well as negative filament tension. We also discuss the creation of spiral and scroll waves during the collision of nonrotating wave fronts. All experiments on three-dimensional media employ optical tomography for the reconstruction of the wave patterns.

I. INTRODUCTION

Far from thermodynamic equilibrium, pattern formation is a common process.[1] A frequently studied case is the propagation of excitation waves in reaction-diffusion media.[2] These nonlinear waves exist in a multitude of physical, chemical, and biological systems. In two-dimensional media, excitation waves can form rotating spiral waves.[3] Experimental examples for these spirals are found in various chemical reactions,[4–6] yeast extracts,[7] aggregating cell colonies,[7] as well as cardiac[8] and neuronal tissue.[9] Typically, these rotors have the shape of Archimedean spirals, and spiral tips describe simple trajectories such as circles. In three-dimensional systems, spiral waves are called scroll waves and rotate around one-dimensional space curves often referred to as "filaments." These filaments are not stationary but move according to their local curvature and gradient in rotation phase.[10,11] Moreover, filaments must terminate at the system boundary, form closed loops, or be pinned to the wake of another wave pulse. The latter option, however, requires that the excitable medium shows a particular type of anomalous dispersion.[12]

The experimental study of three-dimensional excitation waves is hindered by at least two major factors: wave control and wave detection. These technical challenges are particularly problematic in systems such as the mammalian heart, which is nontransparent and in its entirety difficult to control. Nonetheless, a major motivation for the study of three-dimensional excitation waves is related to the heart, where rotating vortex structures are believed to cause cardiac arrhythmia and ventricular fibrillation. This dilemma makes it useful to investigate nonbiological models such as the chemical Belousov–Zhabotinsky (BZ) reaction. The existence of three-dimensional scroll waves in the BZ reaction is well documented.[13,14] However, only a few authors have performed tomographic experiments yielding detailed data on the spatiotemporal evolution of the wave patterns (see, e.g., Refs. 15–17).

In this article, we employ optical tomography for the study of three-dimensional scroll rings in a modified BZ reaction. The critical chemical modification involves the substitution of the classic organic substrate malonic acid with 1,4-cyclohexanedione (CHD). The resulting CHD-BZ system shows a particular feature that is essential for the control of scroll ring nucleation. It relates to the dispersion relation of waves in this system, which describes the velocity of an infinite wave train c as a function of the interpulse spacing λ. In many experimental system, the dispersion relation $c(\lambda)$ is a monotonically increasing function that saturates at the wave speed of the solitary pulse c_0. Moreover, there is al-

a)Author to whom correspondence should be addressed. Electronic mail: steinbck@chem.fsu.edu.

ways a minimal spacing λ_{min} below which no wave trains exist. In the CHD-BZ system, one finds anomalies for which $dc/d\lambda < 0$ and $c(\lambda_{min}) > c_0$. Such systems show transient wave packets in which the trailing pulses propagate faster than the leading front of the packet. Consequently, these pulses approach the back of the frontier pulse. There they undergo a front-to-back collision that results in the annihilation of the trailing pulses. These dynamics have the slightly misleading name "wave merging" and have been studied in detail elsewhere.[18,19] Notice that large-scale wave patterns form despite continuing destruction of pulses because the annihilation zone moves outwards with the leading pulse.

II. EXPERIMENTAL

Propagation of three-dimensional excitation waves is studied in highly viscous Belousov–Zhabotinsky (BZ) systems. The classic BZ reaction involves malonic acid as its organic substrate, which is brominated in the presence of typical redox catalysts such as Ce(III)/Ce(IV) and ferroin/ferriin ($[Fe(phen)_3]^{2+/3+}$). A problem arising from the oxidation of malonic acid and its brominated derivatives is the production of carbon dioxide. This reaction product tends to nucleate gas bubbles, which compromise the spatial homogeneity of the reaction medium and potentially induce undesired fluid flow. Our experiments replace malonic acid with 1,4-cyclohexanedione (CHD). The latter compound is not oxidized to gaseous products and, hence, yields a bubble-free reaction medium. We reemphasize that the use of CHD also causes anomalous dispersion behavior of the traveling waves, which is essential for the specific spiral nucleation scenario to be described in this article.

All experiments are carried out at room temperature. The concentration of sulfuric acid is kept constant at 0.6 M. Furthermore, we use the organometallic complex $[Fe(batho(SO_3)_2)_3]^{3-/4-}$ as catalyst at a concentration of 0.475 mM unless stated otherwise. Notice that the reduced form of this catalyst has a significantly higher molar absorptivity than ferroin.[20] To create a true reaction-diffusion medium without any fluid flow, we increase the viscosity of the reaction solution from about 1 to 150 mPa s by the addition of polyacrylamide solution. The preparation of this polymer solution and all other solutions was described earlier.[12]

We monitor wave patterns based on local changes in the system's absorption of white light. This absorption increases with increasing concentrations of the reduced catalyst. For pseudo-two-dimensional systems, thin layers of the reaction solution are confined between two planar plexiglass plates. For three-dimensional systems, we employ a setup that is shown as a schematic drawing in Fig. 1. About 18–19 mL of the BZ solution are transferred to a cylindrical glass cuvette (inner diameter 3.7 cm). During the measurement, the cuvette is rotated around its symmetry axis using a small electric motor and a simple belt drive. This rotation is critical for our tomographic analysis because it allows us to collect image data from various perspectives. The typical rotation period is 4.9 s.

Image sequences of the rotating sample are recorded with a monochrome charge-coupled device (CCD) camera

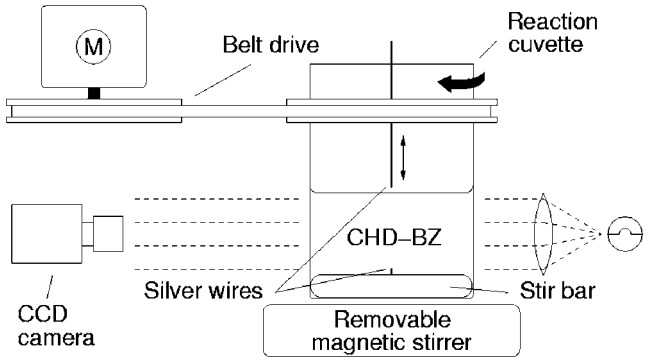

FIG. 1. Schematic drawing of the experimental setup which allows wave detection by optical tomography and the controlled initiation of half-spherical waves using two silver wires. The viscous reaction system can be remixed using a magnetic stir bar. "M" denotes an electric motor which is used to rotate the sample cuvette for detection purposes.

(SONY XC-75). The camera is connected to a PC-based frame grabber board (Data Translation DT 3155) acquiring typically 62 frames per sample rotation. The sample is illuminated with white parallel light. A similar but simpler setup is used to monitor the spatiotemporal evolution of wave patterns in pseudo-two-dimensional media.

III. TOMOGRAPHY

Tomography is an imaging technique that relies on image reconstruction by slices. In the context of concentration patterns in three-dimensional chemical systems, two different types of tomography have been demonstrated in the literature. The first one is magnetic resonance imaging, which, for BZ experiments, exploits differences in the relaxation times of the protons in water.[15] These differences arise from the variation in the local oxidation state of the catalyst and yield good image contrast mainly for the Mn(II)/Mn(III)-catalyzed BZ reaction.[16] The second type of tomography is based on optical-absorption measurements and was pioneered by Winfree *et al.*[17] This article employs the latter approach, which is discussed briefly in the following.

We use filtered back-projection to reconstruct the absorption field $A_{z,t}(x,y)$ in the three-dimensional sample at given height z and time t. This reconstruction is based on image sequences that show the rotating sample at different angles θ which cover 360° in equal steps of $360°/N$ (here $N=62$). A typical example for an individual image of a scroll ring is given in Fig. 2(a). In this snapshot, the gray value in every pixel is the integral of the absorption profile across the sample (i.e., perpendicular to the image plane). The propagating oxidation waves appear as bright bands on a darker, chemically reduced and dynamically excitable, background.

Our computational scheme relies on the slice-wise reconstruction of the full three-dimensional pattern. For this purpose, the image data I are broken into individual sinograms $I_z(x',\theta)$, where z and x' denote the space coordinate along the vertical rotation axis of the sample and the horizontal space coordinate in each snapshot, respectively. A typical example of a sinogram is shown in Fig. 1(b). Our software computes the desired image $I_z(x,y)$ via (1) back-

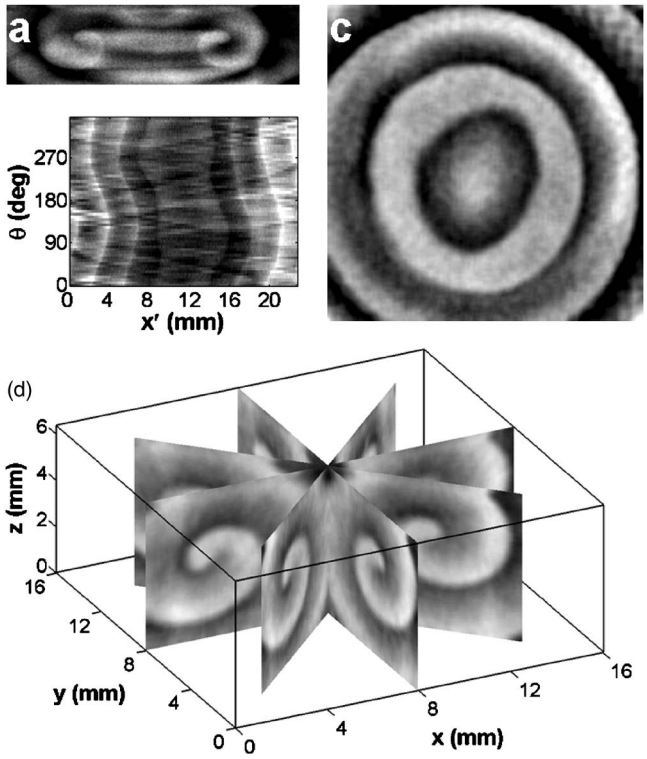

FIG. 2. Tomographic reconstruction of a scroll ring in the CHD-BZ reaction. (a) Single snapshot of the sample during its rotation around a vertical axis. (b) Sinogram obtained by combining absorption profiles at various observation angles θ but constant height z. (c) Absorption in a horizontal slice obtained from the sinogram data using filtered back-projection. (d) Repetition of the reconstruction process at different heights yields the three-dimensional absorption field, which is shown as a fan of slices.

projection of each sinogram along parallel beams of angle θ and (2) summation over all θ. This algorithm is refined by filtering the sinogram data in the frequency domain prior to summation with the specific goal to deemphasize high wave numbers.

The latter procedure creates a reconstruction of the absorption data in a single slice normal to the samples rotation axis. For the example of the scroll ring in Figs. 1(a) and 1(b), these cuts show target-pattern-like structures such as the one in Fig. 1(c). Notice that in Fig. 1(c), the outer ring appears narrower than the inner ring, because the latter is cut in a more tangential fashion. Repetition of the reconstruction for a range of z values yields the desired volume data, which can be rendered using various imaging routines. For example, Fig. 1(d) shows the same scroll ring as a fan of four different cross sections.

IV. RESULTS AND DISCUSSION

Controlled vortex initiation is arguably one of the main challenges for systematic experiments on three-dimensional excitation waves. In two-dimensional systems, spiral wave pairs can be generated according to a number of well established techniques. For example, breaking a continuous wave front creates open wave ends that evolve into spiral rotors. This process can be induced by local mixing[21] or, in the case of photosensitive reactions, by local exposure to bright light.[22] Another strategy is to initiate a wave front in the refractory tail of another wave.[23] If the initiation site is chosen within the so-called "vulnerable" region, initiation in the direction of increasing refractoriness fails and a small C-shaped pattern appears, which evolves into a pair of counter-rotating spirals. Furthermore, spiral waves can also nucleate from planar wave trains rotating around sharply bent obstacles.[24] Unfortunately, these techniques are not readily applicable in three-dimensional systems. For instance, it is very difficult to mix a small, localized volume without disturbing the surrounding medium. Moreover, it is not sufficient to create an essentially point-like open wave end, but one must initialize the filament of the scroll wave by breaking a two-dimensional wave front along a specific, one-dimensional space curve. Ideally one also sets the local phase of spiral rotation along this curve because phase gradients (i.e., the "twist") are important for the subsequent dynamics of the filament.

While some controlled techniques for the initiation of scroll waves have been described in the literature, we still have no satisfying methodology for initiating three-dimensional wave patterns in experiments. For instance, some authors have used glass plates as temporary wave obstacles that once removed can nucleate filaments.[25] However, the removal of the glass plate induces undesired fluid flow or ruptures gel media, which in either case limits the technique's usefulness to simple filaments. Vinson *et al.* created scroll rings by perforating wave fronts with a polyethylene tube or a beam of light.[26] Amemiya *et al.* demonstrated a method that exploits the photosensitivity of the $[Ru(bpy)_3]^{2+}$-catalyzed BZ reaction and the vulnerable region of the refractory wave back.[27] Lastly, Jahnke *et al.* created scroll rings by combining BZ-loaded gel slabs.[28]

Recently, our group began to explore the nucleation of spirals in systems with anomalous wave dispersion using the CHD-BZ reaction as the experimental model.[29] The anomaly of interest allows a trailing wave pulse to propagate faster than its predecessor. This difference in propagation speeds induces a front-to-back collision between the pulses. For appropriate system parameters, the collision results in the annihilation of the trailing pulse. This phenomenon has been named "wave merging" and is also observed in the catalytic reduction of NO with CO on a Pt(100) surface.[30]

Figures 3(a)–3(d) illustrate our method of spiral initiation for a pseudo-two-dimensional CHD-BZ system. The figures show a sequence of four consecutive snapshots. The earliest one (a) reveals three circular, expanding wave fronts that are triggered by small silver wires that locally decrease the concentration of inhibitory bromide via the formation of insoluble silver bromide. Two of the three waves collide in a front-to-front fashion and create a figure-8-shaped envelope wave (b). The third (inner) wave collides with its predecessor front-to-back and annihilates. However, the annihilation is not complete as a small front segment survives within the gap formed by the first wave collision. This segment can be clearly discerned in the middle of Fig. 3(b). Subsequently, its ends curl up and nucleate a pair of counter-rotating spiral waves [Figs. 3(c) and 3(d)]. The distance between the spiral tips remains constant over most of the system's lifetime.

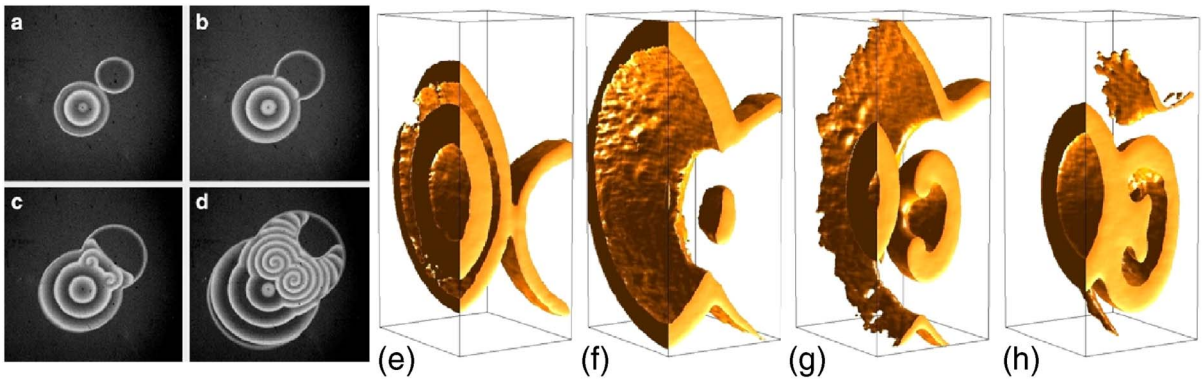

FIG. 3. (Color online) (a)–(d) Consecutive snapshots of merging waves in a thin layer of the CHD-BZ reaction. A pair of spiral waves nucleates from the second wave front emitted by the target pattern. Initial concentrations: [CHD]=0.2 M, [catalyst]=0.5 mM, and [$NaBrO_3$]=0.25 M. Image area: 6:9 cm^2. Time between frames: 27, 33, and 70 s. Reprinted from Ref. 31. (e)–(h) Sequence of tomographically reconstructed wave patterns showing the nucleation of a scroll ring. Initial concentrations: [CHD]=0.185 M and [$NaBrO_3$]=0.18 M. Volume of boxes: $(4.1\times4.1\times9.9)$ mm^3. Time between frames: 38, 19, and 15 s.

The wave dynamics in Figs. 3(a)–3(d) are highly reproducible as long as the annihilation of the third wave does not occur prematurely. It is hence not surprising that this type of spiral nucleation often occurs spontaneously in the CHD-BZ systems resulting in high spiral wave densities. From a technical point of view, it also offers intriguing possibilities for the controlled initiation of scroll waves in three-dimensional systems, because no wave obstacles are involved and the required wave initiation can be readily carried out with silver wires on the surface of the reaction system. In our experiments, initiation is carried out from a permanent silver particle at the bottom of the cuvette and a silver wire that can be lowered onto the solution surface with a micromanipulator. Notice that the former wave source cannot be removed in our setup and, hence, nucleates periodic wave trains. The frequency of these waves, however, is lower than the rotation frequency of the spiral.

An additional problem for experiments with three-dimensional systems stems from undesired waves. They typically nucleate spontaneously upon transfer of the solution to the cuvette and/or after the completion of the system's characteristic induction phase during which it switches from a homogeneously oxidized, unexcitable state to an excitable, chemically reduced state. These undesired waves can be removed efficiently by stirring the reaction solution, which unfortunately rules out the use of gel matrices that are typically used to avoid external and reaction-driven convection. To avoid hydrodynamic flows and also allow for wave-removal by stirring, we increase the BZ solution's viscosity about 150-fold by the addition of polyacrylamide solution. The resulting CHD-BZ system can be remixed using a stir bar that is fitted to the bottom of the reaction cuvette and an external magnetic field (see Fig. 1) which we generate with a conventional stir plate. The aforementioned silver particle is mounted to the center of the stir bar's upper surface. The stir plate is removed prior to rotating the cuvette for tomographic imaging.

Figures 3(e) and 3(f) show a sequence of tomographically reconstructed wave patterns, in which a three-dimensional spiral is created in the collision of essentially spherical wave fronts. Solid (gold colored) regions indicate that locally the catalyst is predominately oxidized, while transparent regions correspond to a chemically reduced medium. To achieve an unobstructed representation of the wave patterns, only the posterior halves of each volume reconstruction are shown. The omitted anterior halves are essentially mirror images of the presented data. We also note that here all three-dimensional reconstructions are rotated positioning the bottom (upper) regions of the cuvette along the left, anterior (right, posterior) surface of the figure boxes. The first snapshot in Fig. 3(e) shows two colliding wave fronts and a third trailing wave. In Fig. 3(f), the frontal collision of the two outer waves has opened up a central hole and the trailing wave has mostly vanished in the refractory zone of its predecessor. However, a small disk-shaped segment of the third wave remains within the central hole. As shown in Figs. 3(g) and 3(h), this disk subsequently curls around its rim and becomes a rotating scroll ring.

In general, scroll rings are three-dimensional spiral waves rotating around closed one-dimensional space curves. These curves are called filaments and are dynamic structures that can move and bend. In the example shown in Figs. 3(g) and 3(h), the filament is a simple circle and spiral rotation along the filament is free of phase gradients. For the given reactant concentrations, the filament shrinks rapidly in the course of spiral rotation and eventually annihilates. This motion is illustrated by the reconstructions in Fig. 4, which show a scroll ring at an early (a) and a late stage (b). The time elapsed between the two frames is 70 s, which equals about two rotation periods of the vortex. During this time, the filament radius decreased from 0.8 to 0.2 mm. Earlier studies showed that the filament remains circular during the collapse and that its radius R changes with a rate proportional to its curvature $dR/dt=-\alpha/R$.[29] The proportionality constant α is known as the filament tension. For the given system, our measurements yield $\alpha=4.2\times10^{-5}$ cm^2/s. The filament also translates in normal direction at a speed of $dz/dt=\beta/R$. The direction of this drift is typically the direction in which the spiral wave propagates through the filament loop ($\beta>0$).

Pairs of counter-rotating scroll rings can be created with a slightly modified initiation protocol. In this protocol, the

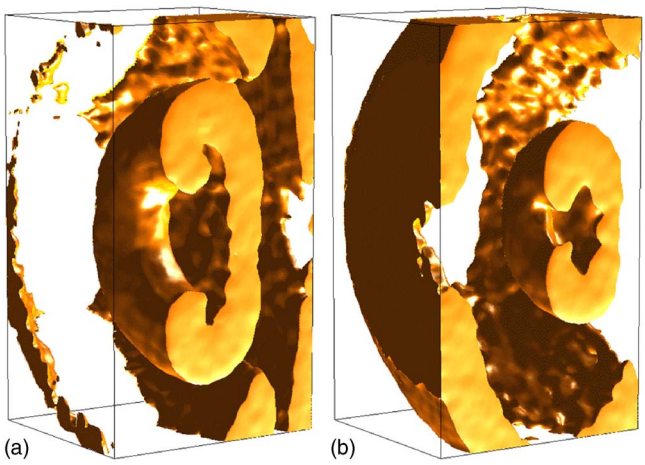

FIG. 4. (Color online) Two consecutive reconstructions of a collapsing and rightward moving scroll ring in the CHD-BZ reaction. Initial concentrations: [CHD]=0.19 M and [$NaBrO_3$]=0.18 M. Volume of boxes: (3.3×2.9×5.8) mm^3. The volume fraction of polyacrylamide solution is 26.3%. Time between frames: 70 s.

upper silver wire is used to create not one but two wave fronts. Figure 5 illustrates such an experiment by showing a sequence of simple gray-level photographs of the reaction system. Notice the trailing wave fronts appear brighter, because the corresponding light is transmitted through four rather than two low-absorption waves and also because the amplitude and width of the first and the second wave pulse are slightly different [cf. Figs. 3(a)–3(d)]. As in the earlier experiment, the outer waves collide and create an hourglass-shaped envelope [Figs. 5(a) and 5(b)] and the trailing waves disappear in the wake of the predecessors [Figs. 5(b) and 5(c)]. Here, however, waves collide also in the equatorial hole region [Figs. 5(c) and 5(d)] frontally and annihilate. The timing of the front-to-front and the front-to-back collisions appears to be slightly asynchronous and two scroll rings are formed. These structures appear as two spiral pairs in Figs. 5(e) and 5(f). The upper scroll ring penetrates its circular filament in a downward direction, while the lower one passes through the filament loop in an upward direction.

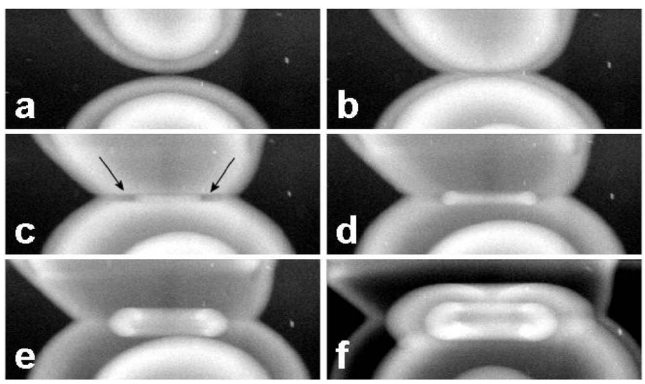

FIG. 5. Image sequence showing the formation of a pair of counter-rotating scroll rings during the collision of four nonrotating, approximately half-spherical wave fronts. The filaments of the vortex pairs are two closely stacked circles. The black arrows in (c) mark small, chemically reduced regions that are connected three-dimensionally along a narrow ring. Initial concentrations: [CHD]=0.19 M and [$NaBrO_3$]=0.185 M. Image area: (13.2×5.0) mm^2. Time between frames: 18, 17, 12, 9, and 35 s.

Although it was observed several times, the highly interesting phenomenon in Fig. 5 is unfortunately very difficult to control and reproduce. This problem leads us to believe that double ring nucleation requires a very precise timing of the wave initiation events and/or small asymmetries of unknown structure. Nonetheless, one can interpret the sparse data that are currently available. These data show that the scroll rings increase their spacing shortly after formation [see Figs. 5(e) and 5(f)]. This motion cannot be explained by the intrinsic vertical motion of single scroll rings as the drift parameter β is positive in this system, which should bring the scroll rings closer to each other. The small opposite motion of the vortex pair and the following absence of vertical drift suggest that parallel, counter-rotating scroll rings repel and hinder each other.

Furthermore, one can speculate what mechanism prevents the complete annihilation of trailing waves and subsequently causes the formation of scroll ring pairs. A possible explanation could lie in an asymmetry that is caused by the velocity-curvature relation of excitation waves. This relation, typically referred to as an eikonal equation, raises (lowers) the speed of concave (convex) fronts proportionally to the front's local curvature.[32] In Figs. 5(a) and 5(b), all fronts are slightly convex with the exception of a cusp-like, circular rim created in the collision of the two outer waves. Along this cusp, the normal velocity is higher and should therefore increase the distance to the trailing wave. Possibly, the small dark regions marked by arrows in Fig. 5(c) are an indication of this increased distance. The buffer zone created might be sufficient to locally delay the front-to-back collision, thus creating open wave ends that swiftly evolve into the observed scroll rings pair.

The dynamics of single scroll rings is not limited to the case of collapsing structures. On the contrary, numerous theoretical and computational studies had predicted negative filament tension and scroll ring expansion. However, the first experimental evidence for this behavior was reported only in 2007.[33] Negative filament tension does not only lead to the expansion of circular filaments but also causes a highly interesting scroll wave instability in which filaments begin to buckle and bend into a highly disordered, dynamic tangle. The latter state is typically referred to as negative filament tension (NT) turbulence or Winfree turbulence.[34,35] The essence of this instability is that small perturbations of the filament shape grow for $\alpha<0$ but vanish for $\alpha>0$.

Figures 6(a) and 6(b) show two consecutive snapshots of a scroll ring in a CHD-BZ system with negative filament tension. For this system, the filament tension was measured as $\alpha=-4.3\times10^{-4}$ cm^2/s.[32] The time elapsed between frames (a) and (b) is 282 s. The vortex structure was initiated using our three-wave technique and showed initially no detectable deviations from an ideal axisymmetric pattern. The frames in Figs. 6(a) and 6(b), however, reveal clear deformations and also show local difference in the phase of spiral rotation. The deformations are more pronounced in frame (b) and, hence, develop in the course of spiral rotation. Furthermore, the distance between the left and right vortex edge, which is

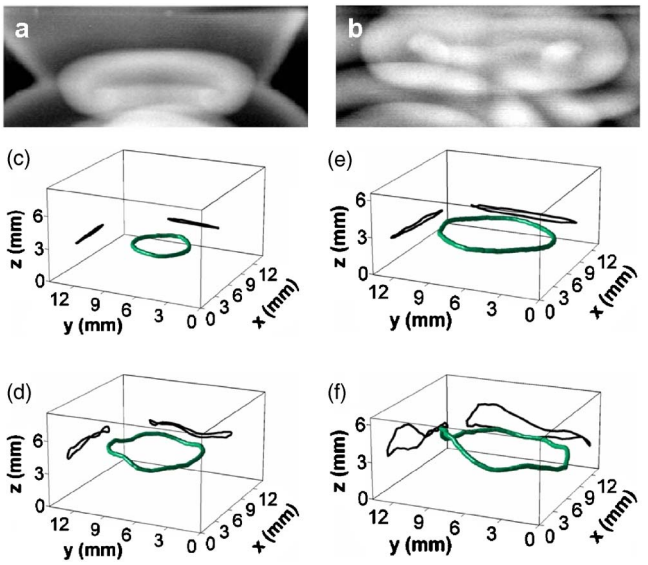

FIG. 6. (Color online) Negative filament tension in the CHD-BZ reaction inducing growth and buckling of initially circular vortex filaments. (a),(b) Two consecutive images of a scroll ring. Image size: (11.0×4.4) mm^2. Time between frames: 282 s. (c),(d) Evolution a small scroll ring filament. Time between frames: 315 s. (d),(e) Evolution a larger scroll ring filament. Time between frames: 432 s. Initial concentrations: [CHD]=0.2 M and [$NaBrO_3$]=0.175 M.

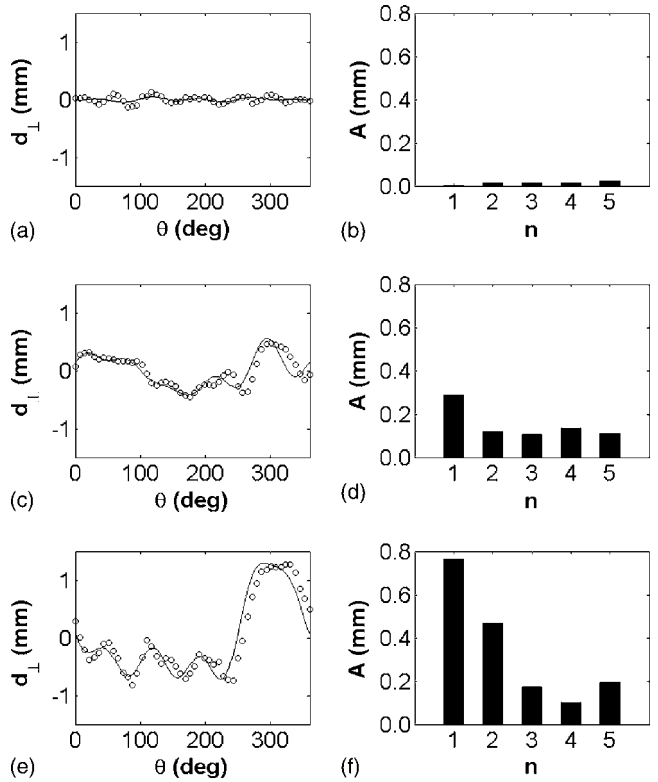

FIG. 7. Left column: Open circles are the measured distances of the filament from its best-fit circle at three consecutive times: (a) 0 s, (b) 154 s, and (c) 432 s. The polar angle θ is defined with respect to the circle's center. The circles' normal vector is fitted only for the initial filament and kept constant for all subsequent data sets. The solid curves are the sums of the corresponding first four Fourier modes. Right column: Plots (d)–(f) show the amplitudes of the first five Fourier modes as computed from the corresponding data in (a)–(c), respectively. Initial concentrations as stated in Fig. 6.

approximately the width of the filament loop, is larger in (b) than in (a).

Figures 6(c)–6(f) show four filaments of scroll rings in the same system. Each frame also contains the filament projections onto the posterior surfaces. The filament coordinates are extracted from three-dimensional reconstructions of the corresponding wave patterns. Frames (c) and (d) illustrate the filament dynamics of an initially small scroll ring. The time elapsed between the two frames is 315 s. Figures 6(e) and 6(f) show similar data for a larger scroll ring. Here, 432 s passed between the frames. In both examples, the later frames (d) and (f) show pronounced deformations while deviations from a simple circle are very small in the early frames (c) and (e). Moreover, a comparison of the later stages suggests that the deformations are stronger for the large scroll ring. This finding is in agreement with our qualitative observation that the bending of circular filaments is delayed, or at least slower, if the filament radius is small.

In an earlier study, we compared the average amplitude of deformations within the filament plane to the one in normal direction. For our experiments, this comparison revealed that, at least initially, out-of-plane deformations are stronger. A typical example for the growth of these out-of-plane deformations is shown in Figs. 7(a)–7(c), where the individual frames are obtained shortly after ring initiation $t=0$ (a), at $t=154$ s (b), and $t=432$ s (c). At a given time, the values of $d_\perp$ are measured as a function the azimuth θ and refer to the distance from the best-fit circle. Notice that the tilt of the circle is kept constant to the orientation of the initial fit while the center and radius vary.

The data in the left column of Fig. 7 are complemented by their corresponding Fourier spectra. The plots (d)–(f) show the amplitude of the first five Fourier modes ($n=1$–5). These modes recover the main features of the distance data as shown by the solid lines in Figs. 7(a)–7(c). For the time interval analyzed, the amplitude of higher modes stays well below 0.1 mm. Notice that all modes have time-dependent wave numbers $k(t)=n/R(t)$, where $R(t)$ denotes the filament radius at time t. We emphasize that the deformations of scroll ring filaments consist of discrete modes ($n\in\mathbb{N}$) because the filament is a closed loop and deformations must be continuous and differentiable. In this specific example, the scroll ring is relatively large and the radius changed only slightly from $R(0\text{ s})=4.7$ mm to $R(432\text{ s})=5.4$ mm. Consequently, the wave numbers of the different modes change only slightly.

The data in Figs. 7(d)–7(f) indicate that the Fourier amplitudes of the first five modes increase in time. This growth is fastest for the mode $n=1$. Figure 8 presents details by plotting the amplitudes of the first three modes as a function of time. The three traces reveal essentially linear dependencies and linear regression yields average growth rates of 1.8, 1.1, and 0.4 μm/s for modes $n=1$–3, respectively. The inset of Fig. 8 shows the temporal evolution of the phase of the first two modes. The data suggest an approximate phase difference of about 90 degrees.

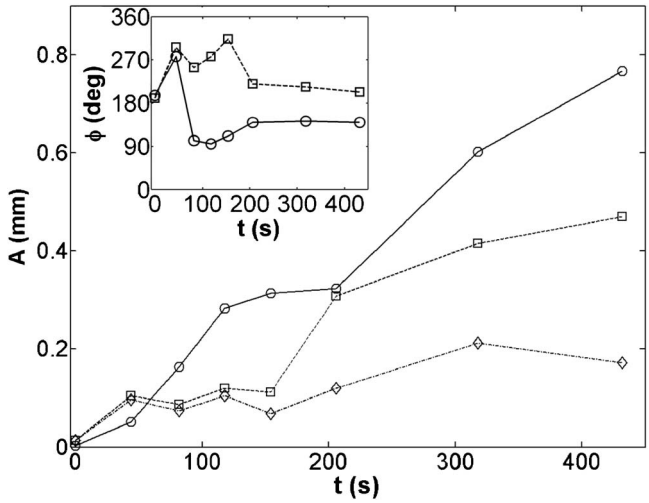

FIG. 8. Amplitude of the first three Fourier modes ($n=1-3$) as a function of time as measured for the expansion of a typical scroll ring. The inset shows the temporal evolution of the Fourier phases for the first two modes. Circles, squares, and diamonds represent data for $n=1$, 2, and 3, respectively. Initial concentrations as stated in Fig. 6.

V. CONCLUSIONS

We have developed experimental methodologies that make the CHD-BZ reaction ideally suited for the study of scroll waves in excitable systems. Specifically, we have shown how anomalous dispersion can be exploited for the controlled initiation of scroll rings. In addition, undesired excitation patterns can be removed prior to vortex initiation, thus allowing cleaner wave experiments. Wave field detection and reconstruction is performed by optical tomography. This method is sufficiently powerful to yield three-dimensional absorption data from which the spatiotemporal evolution of filaments is readily extracted.

The initiation of scroll ring pairs illustrated in Fig. 5 yielded, to our knowledge, the first experimental example for this type of structure. Notice that ring pairs were studied computationally by Bray and Wikso in the specific context of quatrefoil reentry in cardiac systems.[36] Our experiments suggest that the two filament loops of the ring pair repel each other. This conclusion is based on the absence of an expected translation motion that should have decreased the distance between the filaments. Moreover, the filaments did not undergo mutual annihilation, although the latter scenario does not violate the topological constraints governing creation and annihilation events of scroll waves.

Depending on the initial concentrations employed, the CHD-BZ reaction shows positive or negative filament tension. The sign of this parameter is of critical importance to the motion and dynamics of the vortex filament. Specifically for scroll rings, it determines whether the filament loop shrinks or expands. For positive filament tension, we observe ring collapse resulting in the complete annihilation of the vortex. Earlier we showed that the temporal evolution of the filament radius is in excellent agreement with the predicted square root law $R(t)=(R_0-2\alpha t)^{1/2}$, where R_0 denotes the radius at time $t=0$.[29] Here, we examined the case of negative filament tension more closely showing that ring expansion is accompanied by growing deformations of the initially circular filament. These deformations are predicted to result in a turbulent state.[34,35] The latter shares qualitative similarities with vortex line turbulence in hydrodynamics. However, filaments in the CHD-BZ reaction and similar excitable media are not known to intersect each other.

While it is currently difficult to access the fully developed turbulent state experimentally, we have presented details on the early growth of different deformation modes for the specific case of scroll rings. This case differs from waves with linear filaments, because deformation spectra on filament loops are quantized. Our results show that the deformations of circular filaments with mm-sized radii grow fastest for the modes $n=1-3$ and are initially inactive for $n>5$ (Figs. 7 and 8). This observation can be discussed in the context of theoretical work by Henry and Hakim,[37,38] who investigated the linear stability of scroll waves with straight filaments. For NT conditions, it was found that the growth rates are negative for perturbations with large wave numbers and positive in a finite band of small wave numbers. Disregarding curvature and quantization effects, one can speculate whether the active modes in our data are within the latter band, while all other modes are inactive due to negative growth rates.

Clearly more work is needed to explore the interesting problem of quantized scroll ring instabilities. It seems reasonable to assume that experimental investigations like ours will provide new ideas as well as useful test cases for future theoretical analyses of scroll wave instabilities, NT turbulence, and filament interaction. We also believe that chemical models of three-dimensional excitable media will continue to accompany biophysical investigations on cardiac systems in a fruitful fashion as they allow for more systematic and quantitative exploration.

ACKNOWLEDGMENTS

This material is based on work supported by the National Science Foundation under Grant No. 0513912.

[1]M. C. Cross and P. C. Hohenberg, "Pattern formation outside of equilibrium," Rev. Mod. Phys. **65**, 851 (1993).
[2]E. Meron, "Pattern formation in excitable media," Phys. Rep. **218**, 1 (1992).
[3]D. Barkley, "Euclidian symmetry and the dynamics of rotating spiral waves," Phys. Rev. Lett. **72**, 164 (1994).
[4]A. T. Winfree, "Spiral waves of chemical activity," Science **175**, 634 (1972).
[5]V. K. Vanag and I. R. Epstein, "Segmented spiral waves in a reaction-diffusion system," Proc. Natl. Acad. Sci. U.S.A. **100**, 14635 (2003).
[6]K. Agladze and O. Steinbock, "Waves and vortices of rust on the surface of corroding steel," J. Phys. Chem. A **104**, 9816 (2000).
[7]S. C. Müller, T. Mair, and O. Steinbock, "Traveling waves in yeast extracts and in cultures of Dictyostelium discoideum," Biophys. Chem. **72**, 37 (1998).
[8]Focus issue: Cardiovascular Physics, Chaos **17**, 015101–015121 (2007).
[9]M. A. Dahlem and S. C. Müller, "Reaction-diffusion waves in neuronal tissue and the window of cortical excitability," Ann. Phys. **13**, 442 (2004).
[10]J. P. Keener, "The dynamics of 3-dimensional scroll waves in excitable media," Physica D **31**, 269 (1988).
[11]B. Echebarria, V. Hakim, and H. Henry, "Nonequilibrium ribbon model of twisted scroll waves," Phys. Rev. Lett. **96**, 098301 (2006).
[12]T. Bánsági, Jr., C. Palczewski, and O. Steinbock, "Scroll wave filaments

terminate in the back of traveling fronts," J. Phys. Chem. A **111**, 2492 (2007).
[13]A. T. Winfree, "Scroll-shaped waves of chemical activity in 3 dimensions," Science **181**, 937 (1973).
[14]B. J. Welsh, J. Gomatam, and A. E. Burgess, "3 dimensional chemical waves in the Belousov–Zhabotinskii reaction," Nature **304**, 611 (1983).
[15]A. F. Taylor and M. M. Britton, "Magnetic resonance imaging of chemical waves in porous media," Chaos **16**, 037103 (2006).
[16]A. L. Cross, R. L. Armstrong, C. Gobrecht, M. Panton, and C. Ware, "Contrast enhancement of magnetic resonance images of chemical waves in the Belousov–Zhabotinsky reaction," J. Phys. Chem. **99**, 16616 (1995).
[17]A. T. Winfree, S. Caudle, G. Chen, P. McGuire, and Z. Szilagyi, "Quantitative optical tomography of chemical waves and their organizing centers," Chaos **6**, 617 (1996).
[18]N. Manz, S. C. Müller, and O. Steinbock, "Anomalous dispersion of chemical waves in a homogeneously catalyzed reaction system," J. Phys. Chem. A **104**, 5895 (2000).
[19]C. T. Hamik, N. Manz, and O. Steinbock, "Anomalous dispersion and attractive pulse interaction in the 1,4-cyclohexanedione Belousov–Zhabotinsky reaction," J. Phys. Chem. A **105**, 6144 (2001).
[20]B. T. Ginn, B. Steinbock, M. Kahveci, and O. Steinbock, "Microfluidic devices for the Belousov–Zhabotinsky reaction," J. Phys. Chem. A **108**, 1325 (2004).
[21]K. I. Agladze and V. I. Krinsky, "Multi-armed vortices in an active chemical medium," Nature **296**, 424 (1982).
[22]O. Steinbock and S. C. Müller, "Chemical spiral rotation is controlled by light-induced artificial cores," Physica A **188**, 61 (1992).
[23]R. Tóth, V. Gáspár, A. Belmonte, M. C. O'Connell, A. Taylor, and S. K. Scott, "Wave initiation in the ferroin-catalysed Belousov–Zhabotinsky reaction with visible light," Phys. Chem. Chem. Phys. **2**, 413 (2000).
[24]K. Agladze, J. P. Keener, S. C. Müller, and A. Panfilov, "Rotating spiral waves created by geometry," Science **264**, 1746 (1994).
[25]U. Storb, C. R. Neto, M. Bär, and S. C. Müller, "A tomographic study of desynchronization and complex dynamics of scroll waves in an excitable chemical reaction with a gradient," Phys. Chem. Chem. Phys. **5**, 2344 (2003).
[26]M. Vinson, S. Mironov, S. Mulvey, and A. Pertsov, "Control of spatial orientation and lifetime of scroll rings in excitable media," Nature **386**, 477 (1997).
[27]T. Amemiya, S. Kádár, P. Kettunen, and K. Showalter, "Spiral wave formation in three-dimensional excitable media," Phys. Rev. Lett. **77**, 3244 (1996).
[28]W. Jahnke, C. Henze, and A. T. Winfree, "Chemical vortex dynamics in three-dimensional excitable media," Nature **336**, 662 (1988).
[29]T. Bánsági, Jr. and O. Steinbock, "Nucleation and collapse of scroll rings in excitable media," Phys. Rev. Lett. **97**, 198301 (2006).
[30]J. Christoph, M. Eiswirth, N. Hartmann, R. Imbihl, I. Kevrekidis, and M. Bär, "Anomalous dispersion and pulse interaction in an excitable surface reaction," Phys. Rev. Lett. **82**, 1586 (1999).
[31]N. Manz, C. T. Hamik, and O. Steinbock, "Tracking waves and vortex nucleation in excitable systems with anomalous dispersion," Phys. Rev. Lett. **92**, 248301 (2004).
[32]A. S. Mikhailov, *Foundations of Synergetics I. Distributed Active Systems* (Springer, New York, 1991).
[33]T. Bánsági, Jr. and O. Steinbock, "Negative filament tension of scroll rings in an excitable system," Phys. Rev. E **76**, 045202 (2007).
[34]S. Alonso, F. Sagues, and A. S. Mikhailov, "Taming Winfree turbulence of scroll waves in excitable media," Science **299**, 1722 (2003).
[35]R. M. Zaritski, S. F. Mironov, and A. M. Pertsov, "Intermittent self-organization of scroll wave turbulence in three-dimensional excitable media," Phys. Rev. Lett. **92**, 168302 (2004).
[36]M. A. Bray and J. P. Wikswo, "Interaction dynamics of a pair of vortex filament rings," Phys. Rev. Lett. **90**, 238303 (2003).
[37]H. Henry and V. Hakim, "Linear stability of scroll waves," Phys. Rev. Lett. **85**, 5328 (2000).
[38]H. Henry and V. Hakim, "Scroll waves in isotropic excitable media: Linear instabilities, bifurcations, and restabilized states," Phys. Rev. E **65**, 046235 (2002).